

Analysis of a Thyristor Chopper Circuit of Forced Commutation Type

By

Jūrō UMOTO* and Osamu NAKAMURA*

(Received December 23, 1969)

In this paper, we investigate theoretically and experimentally a thyristor chopper circuit of forced commutation type, which is named the oscillation circuit type chopper. Considering the power source inductance and the internal resistances of circuit elements, we analyze the chopper circuit strictly, compare the digital computation results with the experimental ones and find numerically the optimum circuit conditions.

1. Introduction

As in recent years we can produce the thyristors of good characteristics and big capacity, chopper circuits with the thyristors are used extensively as variable d.c. power source, especially for speed control of d.c. motors¹⁾.

Thyristor chopper circuits are the ones which control the d.c. power that is supplied to the load, by interrupting it by means of a thyristor. We can classify the circuits into the self-commutation- and the forced-commutation-types. The former is represented by the Morgan circuit^{2,3)}, and the latter by the Jones circuit and the oscillation circuit type chopper^{4,5)}. As the Morgan circuit does not need an auxiliary commutation thyristor, the trigger circuit can be simplified, but since the on-time of the main thyristor is determined by the circuit constants, in the case of the fixed repetition frequency, the on-time control is complicated. The Jones circuit is stable for load fluctuations, but it has the defect that the saturable auto-transformer conducts main current and so the optimum operating frequency becomes low. On the other hand, the oscillation circuit has the advantages that the main thyristor only conducts the main current, the circuit can operate till the relative high frequency and it presents stable transient performances.

Now as strict analyses of the oscillation circuit type chopper have not been done, in which are considered all the modes to appear in the circuit, in this paper

* Department of Electrical Engineering.

considering the power source inductance and the internal resistance of every element, etc. with respect to the thyristor chopper, we derive theoretically exact solutions of the fundamental circuit equations, compare the digital computation results with the experimental ones and discuss the characteristics of the circuit.

2. Theoretical Analysis

2.1 Working Modes

Fig. 1 shows a chopper circuit, which is called the oscillation circuit type chopper. In this circuit,

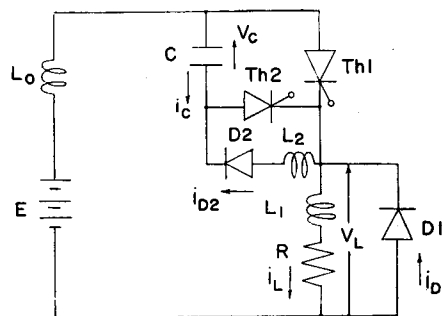


Fig. 1. Oscillation circuit type chopper.

Th1 and *Th2* : main and auxiliary commutation thyristors,

D1 and *D2* : diodes,

L_0 : power source inductance,

L_2 : inductance,

L_1 and R : load inductance and resistance,

C : capacitance,

E : d.c. power source voltage,

v_L and i_L : load voltage and current,

v_C and i_C : condenser voltage and current,

i_{D1} and i_{D2} : currents through *D1* and *D2*.

Next Fig. 2 (a) to (h) illustrate every circuit mode, which the circuit in Fig. 1 gives. Namely

Mode I : *Th1* is gated on in the situation that C is charged positively, the d.c. power is supplied to the load from the source and in this duration the polarity of v_C is reversed.

Mode II : v_C is kept negative by *D2*, and meanwhile the source is supplying the power to the load through *Th1*.

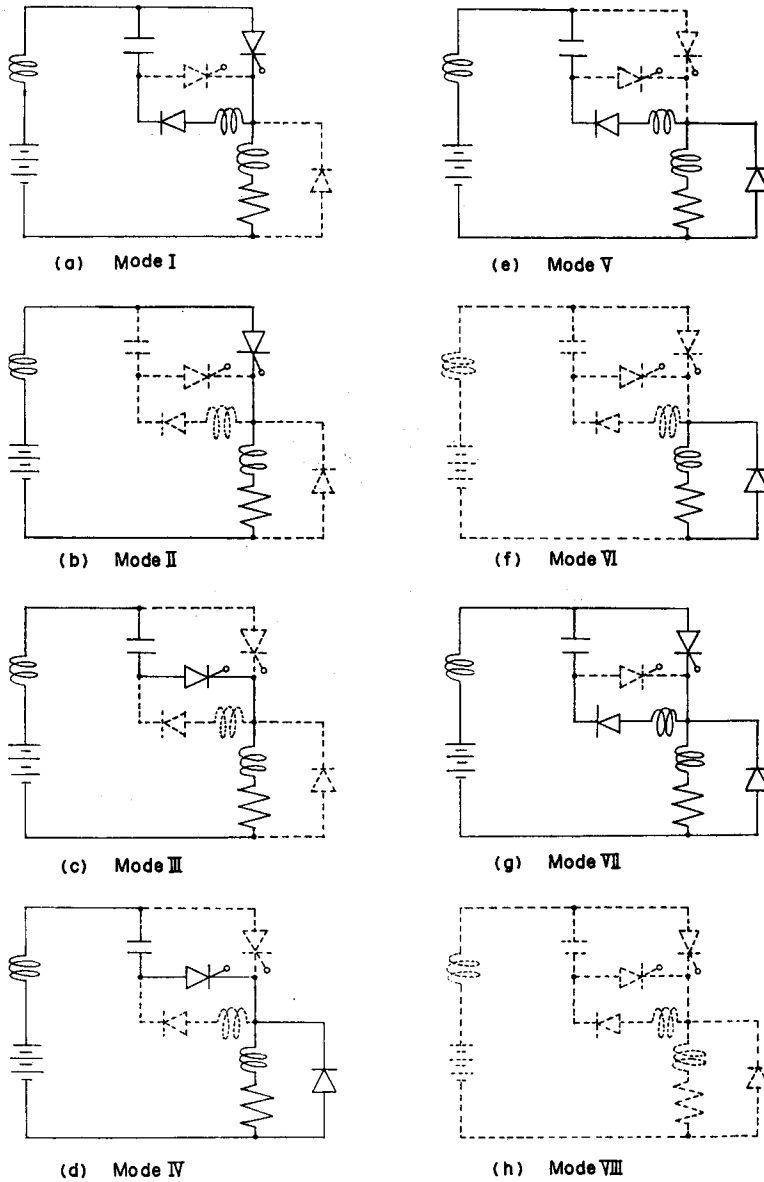
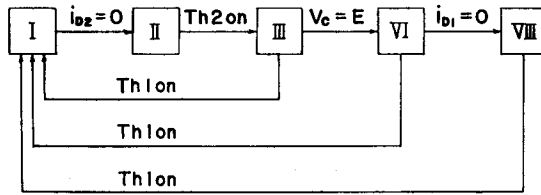


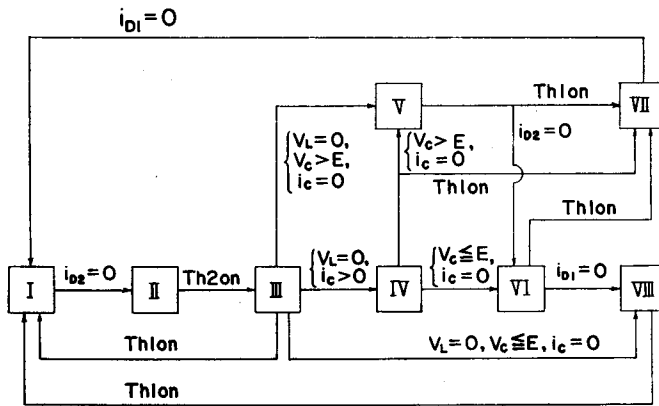
Fig. 2. Situation of every circuit mode.

Mode III : Th_2 is triggered, v_c appears as inverse voltage across Th_1 , hence Th_1 is turned off and C is charged positively again.

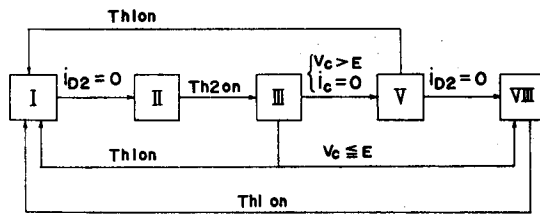
Mode IV : if in mode III v_L decreases to zero and D_1 conducts the current, mode IV comes about while i_c is flowing. This mode exists in the case, where the conductive portion in mode III becomes



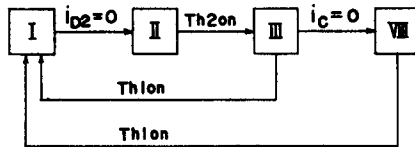
(a) $L_0=0, L_1 \neq 0$



(b) $L_0 \neq 0, L_1 \neq 0$



(c) $L_0 \neq 0, L_1 = 0$



(d) $L_0=0, L_1=0$

Fig. 3. Mode transitions and criteria.

oscillatory by L_0 and C . In transition from mode III to IV, i_c can not drop to zero discontinuously due to L_0 . In this interval, v_c is higher than E .

Mode V : in consequence that v_c is higher than E and the circuit oscillatory by L_0 and C , i_c flows toward the source inversely. $Th 2$ turns off because of its inverse voltage. At the end of this mode, v_c becomes lower than E .

Mode VI : charging current i_c , which is going to flow once again, is checked by $D 2$ and i_c circulates through $D 1$ due to the existence of L_1 .

Mode VII : in the case where $Th 1$ is gated on in mode IV, V or VI, mode VII presents itself as the transient state before moving to mode I.

Mode VIII: the situation that all thyristors and diodes are off.

Next, we show the mode transitions and the criteria in Fig. 3.

2.2 Fundamental Circuit Equations and Their Solutions

The fundamental differential equations for all circuit modes shown in Fig. 2 become as follows:

for mode I:

$$\left. \begin{aligned} E &= (L_0 + L_1) \frac{di_{L1}}{dt} + (R + r_1)i_{L1} + r_6 i_{D21}, \\ i_{C1} &= C \frac{dv_{C1}}{dt}, \\ v_{C1} &= L_2 \frac{di_{D21}}{dt} + r_2 i_{D21} + r_6 i_{L1}, \\ i_{C1} + i_{D21} &= 0, \\ i_{D11} &= 0, \end{aligned} \right\} \quad (1)$$

for mode II:

$$\left. \begin{aligned} E &= (L_0 + L_1) \frac{di_{L2}}{dt} + (R + r_1)i_{L2}, \\ i_{C2} &= 0, \\ C \frac{dv_{C2}}{dt} &= 0, \\ i_{D12} &= 0, \\ i_{D22} &= 0, \end{aligned} \right\} \quad (2)$$

for mode III:

$$\left. \begin{aligned} E &= (L_0 + L_1) \frac{di_{L3}}{dt} + (R + r_3)i_{L3} + v_{C3}, \\ i_{L3} - i_{C3} &= 0, \end{aligned} \right\} \quad (3)$$

$$\left. \begin{aligned} i_{C3} &= C \frac{dv_{C3}}{dt}, \\ i_{D13} &= 0, \\ i_{D23} &= 0, \end{aligned} \right\}$$

for mode IV :

$$\left. \begin{aligned} E &= L_0 \frac{di_{C4}}{dt} + r_3 i_{C4} - r_4 i_{D14} + v_{C4}, \\ i_{C4} &= C \frac{dv_{C4}}{dt}, \\ Ri_{L4} + L_1 \frac{di_{L4}}{dt} + r_4 i_{D14} &= 0, \\ i_{D14} + i_{C4} - i_{L4} &= 0, \\ i_{D24} &= 0, \end{aligned} \right\} \quad (4)$$

for mode V :

$$\left. \begin{aligned} E &= -(L_0 + L_2) \frac{di_{D25}}{dt} - r_4 i_{D15} - r_5 i_{D25} + v_{C5}, \\ i_{C5} &= C \frac{dv_{C5}}{dt}, \\ Ri_{L5} + L_1 \frac{di_{L5}}{dt} + r_4 i_{D15} &= 0, \\ i_{C5} + i_{D25} &= 0, \\ i_{D15} - i_{D25} - i_{L5} &= 0, \end{aligned} \right\} \quad (5)$$

for mode VI :

$$\left. \begin{aligned} (R + r_4) i_{L6} + L_1 \frac{di_{L6}}{dt} &= 0, \\ i_{C6} &= 0, \\ C \frac{dv_{C6}}{dt} &= 0, \\ i_{D16} - i_{L6} &= 0, \\ i_{D26} &= 0, \end{aligned} \right\} \quad (6)$$

for mode VII :

$$\left. \begin{aligned} E &= L_0 \frac{d}{dt} (i_{L7} - i_{D17}) + r_1 (i_{L7} - i_{D17}) - r_4 i_{D17} + r_6 i_{D27}, \\ i_{C7} &= C \frac{dv_{C7}}{dt}, \\ Ri_{L7} + L_1 \frac{di_{L7}}{dt} + r_4 i_{D17} &= 0, \\ i_{C7} + i_{D27} &= 0, \\ v_{C7} &= L_2 \frac{di_{D27}}{dt} + r_2 i_{D27} + r_6 (i_{L7} - i_{D17}), \end{aligned} \right\} \quad (7)$$

for mode VIII :

$$\left. \begin{aligned} i_{L8} &= 0, \\ i_{C8} &= 0, \\ C \frac{dv_{C8}}{dt} &= 0, \\ i_{D18} &= 0, \\ i_{D28} &= 0, \end{aligned} \right\} \quad (8)$$

where

added suffixes 1 to 8: show the mode number,

$$r_1 = r_{Th1} + r_{L0}, \quad r_2 = r_{Th2} + r_{D2} + r_C + r_{L2},$$

$$r_3 = r_{Th2} + r_{L0} + r_C, \quad r_4 = r_{D1},$$

$$r_5 = r_{D2} + r_{L0} + r_C + r_{L2}, \quad r_6 = r_{Th1},$$

r_{Th1} and r_{Th2} : internal resistance of $Th1$ and $Th2$,

r_{D1} and r_{D2} : internal resistances of $D1$ and $D2$,

r_{L0} and r_{L2} : internal resistances of L_0 and L_2 ,

r_C : resistance for measurement of i_C ,

and after solving $i_L(t)$ with the fundamental equations, the load voltage $v_L(t)$ is obtained by

$$v_L(t) = L_1 \frac{di_L(t)}{dt} + R i_L(t). \quad (9)$$

Next applying the Laplace transformation to the fundamental circuit equations (1) to (8) and considering the mode changes illustrated in Fig.3 and the stage number, the solutions of voltages and currents are given in the following matrix forms.

$$[w_{rn}(s)] = [\varphi_r(s)] + [X_r(s)][w_{rn}^{-0}], \quad (10)$$

where

$$\left. \begin{aligned} [w_{rn}(s)] &= \begin{pmatrix} i_{Lrn}(s) \\ i_{Crn}(s) \\ v_{Crn}(s) \\ i_{D1rn}(s) \\ i_{D2rn}(s) \end{pmatrix} \\ [w_{rn}^{-0}] &: \text{initial value matrix of} \\ &\quad \text{first kind of } [w_{rn}(t)], \\ r &= 1, 2, \dots, 8: \text{mode number,} \\ n &= 1, 2, \dots: \text{stage number,} \\ s &: \text{Laplace operator.} \end{aligned} \right\} \quad (10)$$

Then by applying the inverse Laplace transformation to Eq. (10), we have

$$[w_{rn}(t)] = [\varphi_r(t)] + [X_r(t)][w_{rn}^{-0}] \quad (11)$$

As it is troublesome to describe $[\varphi_r(t)]$'s and $[\mathcal{X}_r(t)]$'s of all modes, let us show only the theoretical results for the case of $\lambda < 1$ in mode III. For mode III, Eq. (11) is given by

$$\begin{pmatrix} i_{L3}(t) \\ i_{C3}(t) \\ v_{C3}(t) \\ i_{D13}(t) \\ i_{D23}(t) \end{pmatrix} = [\varphi_3(t)] + [\mathcal{X}_3(t)] \begin{pmatrix} i_{L3}^{-0} \\ i_{C3}^{-0} \\ v_{C3}^{-0} \\ i_{D13}^{-0} \\ i_{D23}^{-0} \end{pmatrix}, \tag{12}$$

where suffix r is omitted and

$$\left. \begin{aligned} [\varphi_3(t)] &= \begin{pmatrix} \varphi_{13}(t) \\ \varphi_{23}(t) \\ \varphi_{33}(t) \\ 0 \\ 0 \end{pmatrix}, \\ [\mathcal{X}_3(t)] &= \begin{pmatrix} \mathcal{X}_{113}(t) & 0 & \mathcal{X}_{133}(t) & 0 & 0 \\ \mathcal{X}_{213}(t) & 0 & \mathcal{X}_{233}(t) & 0 & 0 \\ \mathcal{X}_{313}(t) & 0 & \mathcal{X}_{333}(t) & 0 & 0 \\ 0 & 0 & 0 & 0 & 0 \\ 0 & 0 & 0 & 0 & 0 \end{pmatrix}, \end{aligned} \right\} \tag{12}'$$

in which for the case, in which $\lambda = \frac{R+r_3}{2} \sqrt{\frac{C}{L_0+L_1}} < 1$, namely the circuit is oscillatory,

$$\left. \begin{aligned} \varphi_{13}(t) &= \frac{E}{L_0+L_1} \frac{\varepsilon^{-\lambda t}}{\nu\sqrt{1-\lambda^2}} \sin(\nu\sqrt{1-\lambda^2} t), \\ \varphi_{23}(t) &= \varphi_{13}(t), \\ \varphi_{33}(t) &= E \left[1 - \varepsilon^{-\lambda t} \left\{ \frac{\lambda}{\sqrt{1-\lambda^2}} \sin(\nu\sqrt{1-\lambda^2} t) + \cos(\nu\sqrt{1-\lambda^2} t) \right\} \right], \\ \mathcal{X}_{113}(t) &= \varepsilon^{-\lambda t} \left\{ \cos(\nu\sqrt{1-\lambda^2} t) - \frac{\lambda}{\sqrt{1-\lambda^2}} \sin(\nu\sqrt{1-\lambda^2} t) \right\}, \\ \mathcal{X}_{213}(t) &= \mathcal{X}_{113}(t), \\ \mathcal{X}_{313}(t) &= \frac{\varepsilon^{-\lambda t}}{C\nu\sqrt{1-\lambda^2}} \sin(\nu\sqrt{1-\lambda^2} t), \\ \mathcal{X}_{133}(t) &= -\frac{1}{L_0+L_1} \frac{\varepsilon^{-\lambda t}}{\nu\sqrt{1-\lambda^2}} \sin(\nu\sqrt{1-\lambda^2} t), \\ \mathcal{X}_{233}(t) &= \mathcal{X}_{133}(t), \\ \mathcal{X}_{333}(t) &= \varepsilon^{-\lambda t} \left\{ \cos(\nu\sqrt{1-\lambda^2} t) + \frac{\lambda}{\sqrt{1-\lambda^2}} \sin(\nu\sqrt{1-\lambda^2} t) \right\}, \\ \nu &= 1/\sqrt{C(L_0+L_1)}. \end{aligned} \right\} \tag{12}''$$

In this connection,

$$\begin{aligned}
 v_{L3}(t) &= L_1 \frac{di_{L3}(t)}{dt} + Ri_{L3}(t) \\
 &= \frac{EL_1}{L_0 + L_1} \varepsilon^{-\lambda t} \left\{ \cos(\nu\sqrt{1-\lambda^2} t) + \frac{-\lambda\nu + R/L_1}{\nu\sqrt{1-\lambda^2}} \sin(\nu\sqrt{1-\lambda^2} t) \right\} \\
 &\quad + i_{L3}^{-0} \varepsilon^{-\lambda t} \left[\left\{ R - \frac{L_1(R+r_3)}{L_0 + L_1} \right\} \cos(\nu\sqrt{1-\lambda^2} t) + \frac{\lambda}{\sqrt{1-\lambda^2}} \right. \\
 &\quad \times \left. \left\{ -R + \frac{L_1(R+r_3)}{L_0 + L_1} - \frac{2L_1}{C(R+r_3)} \right\} \sin(\nu\sqrt{1-\lambda^2} t) \right. \\
 &\quad \left. + v_{C3}^{-0} \varepsilon^{-\lambda t} \frac{L_1}{L_0 + L_1} \left\{ -\cos(\nu\sqrt{1-\lambda^2} t) + \frac{\lambda\nu - R/L_1}{\nu\sqrt{1-\lambda^2}} \sin(\nu\sqrt{1-\lambda^2} t) \right\} \right].
 \end{aligned} \tag{13}$$

In the same way we can get $[\varphi(t)]$'s and $[\chi(t)]$'s of the other modes.

Next the initial value matrix $[w_{rn}^{-0}]$ can be determined by means of the analytical method of the periodically interrupted electric circuit of the third genus. Namely from Eq. (11) and Fig. 4, where t_r 's ($r=1, 2, \dots, 7$) express the duration of the interval of the r -th mode, we can derive the following equations,

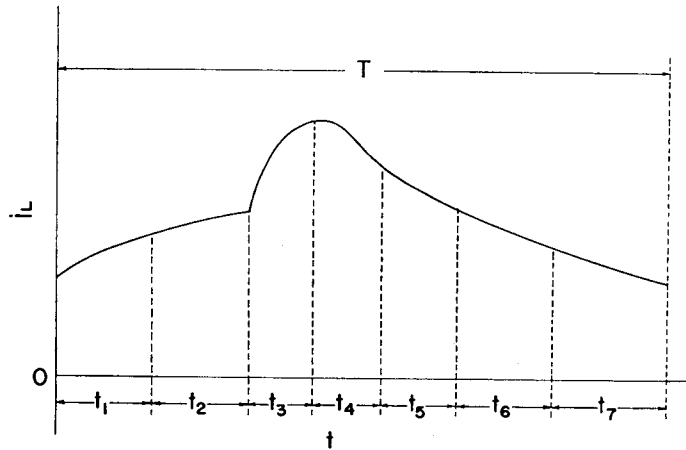


Fig. 4. Duration of interval of each mode.

$$\begin{aligned}
 [w_{rn}^{-0}] &= [\varphi_{r-1, n}] + [\chi_{r-1, n}] [\varphi_{r-2, n}] + [\chi_{r-1, n}] [\chi_{r-2, n}] [\varphi_{r-3, n}] + \dots \\
 &\quad \dots + [\chi_{r-1, n}] [\chi_{r-2, n}] \dots [\chi_1, n] [\chi_7, n-1] \dots [\chi_r, n-1] [w_{r, n-1}^{-0}], \\
 [w_{r, n-1}] &= [\varphi_{r-1, n-1}] + [\chi_{r-1, n-1}] [\varphi_{r-2, n-1}] + \dots \\
 &\quad \dots + [\chi_{n-1, n-1}] [\chi_{r-2, n-1}] \dots [\chi_1, n-1] [\chi_7, n-2] \dots [\chi_r, n-2] [w_{r, n-2}^{-0}] \\
 &\quad \dots \\
 &\quad \dots \\
 [w_{r, 2}^{-0}] &= [\varphi_{r-1, 2}] + [\chi_{r-1, 2}] [\varphi_{r-2, 2}] + \dots \\
 &\quad \dots + [\chi_{r-1, 2}] [\chi_{r-2, 2}] \dots [\chi_{12}, 2] [\chi_{71}, 2] \dots [\chi_{r1}, 2] [w_{r1}^{-0}],
 \end{aligned} \tag{14}$$

where

$$\left. \begin{aligned} [w_{r1}^{-0}] &= [\varphi_{r-1,1}] + [\chi_{r-1}][\varphi_{r-2,1}] + \dots + [\chi_{r-1,1}][\chi_{r-2,1}] \dots [\chi_{21}][w_{11}^{-0}], \\ [w_{12}^{-0}] &= [\varphi_{71}] + [\chi_{71}][\varphi_{61}] + \dots + [\chi_{71}][\chi_{61}] \dots [\chi_{21}][w_{11}^{-0}], \\ [\varphi_{jk}] &= [\varphi_j(t_{jk})], \\ [\chi_{jk}] &= [\chi_j(t_{jk})], \\ j &= 1, 2, \dots, r, \dots, 7, \\ k &= 1, 2, \dots, n, \dots \end{aligned} \right\} (14)$$

Therefore if we give numerically the initial value matrix of the first stage and the first mode, we can calculate the numerical values of the voltages and currents at an arbitrary instant by using Eq. s (11) and (14).

3. Numerical Calculations and Experimental Results

As described in Section 2.2, we can numerically calculate the values of the voltages and currents at an arbitrary time, when we give the numerical values of the elements of $[w_{11}^{-0}]$, namely the starting values of the voltages and currents. But since the duration of each mode is affected by the magnitudes of voltages and currents, it is impossible to get theoretically the duration of each mode. So let us use the iteration method, which is very practical for a digital computer. It is the method, in which after providing numerically the elements of $[w_{11}^{-0}]$, at each calculation time step the criterion of a mode transition are checked, and if the criterion is satisfied, the final values of every voltage and current in the mode are used as the initial ones in the next mode, and if such a way is continued and every voltage and current reach the state, which we can regard as the steady one, the numerical computation is stopped. By this method the circuit in Fig. 1 can be simulated with a digital computer, and we can numerically obtain the values of the voltages and currents at an arbitrary instant and for an arbitrary circuit conditions. Fig. 5 illustrates the digital computer flow-chart.

Now we carry out the numerical calculations with the following combinations of circuit parameters,

- i) $C = 1 \sim 30 \mu\text{F}$
 $L_0 = 0 \text{ mH}$,
 L_1 : parameter,
 $r_{L_0} = 0 \Omega$,
- ii) $C = 5 \mu\text{F}$,
 $L_0 = 0 \sim 40 \text{ mH}$,
 L_1 : parameter,
 r_{L_0} : depends on L_0

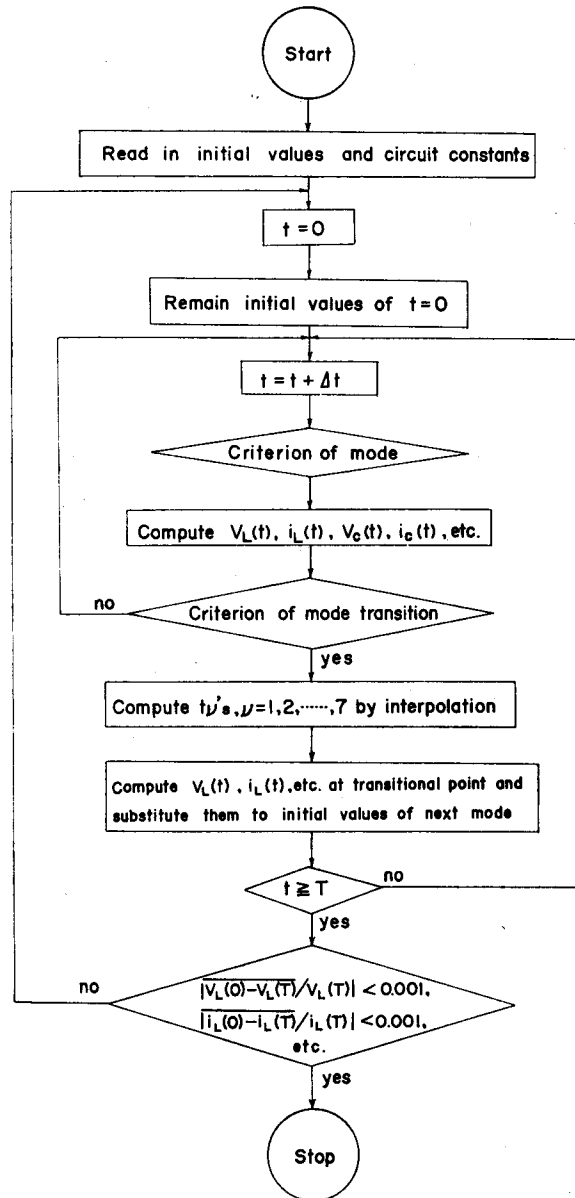


Fig. 5. Digital computer flow-chart.

where the values of the following quantities are assumed as constant, namely

$$\begin{array}{lll}
 E=50 \text{ V}, & T=5 \text{ ms}, & T_{on}=2 \text{ ms}, \\
 R=50 \Omega, & L_2=10 \text{ mH}, & r_{Th1}=1.7 \Omega, \\
 r_{Th2}=1.2 \Omega, & r_C=0.5 \Omega, & r_{D1}=1.7 \Omega \\
 r_{D2}=1.7 \Omega & \text{and} & r_{L2}=2.0 \Omega.
 \end{array}$$

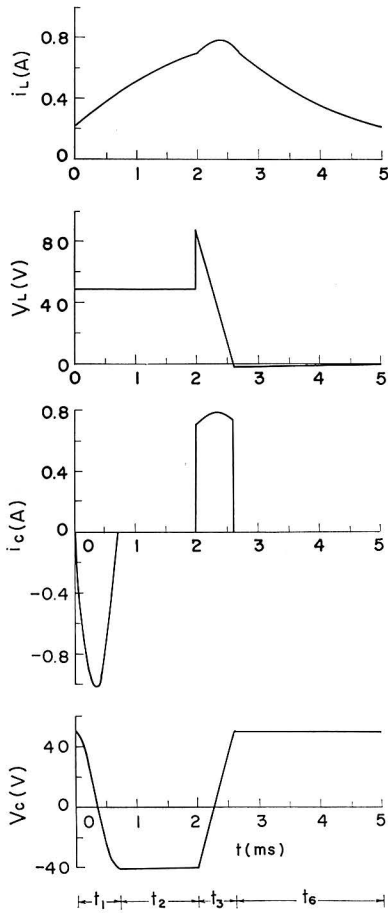


Fig. 6. Calculated waveforms of i_L , v_L , i_C and v_C when $C=5 \mu\text{F}$, $L_0=0 \text{ mH}$, $L_1=100 \text{ mH}$ and $r_{L0}=0 \Omega$.

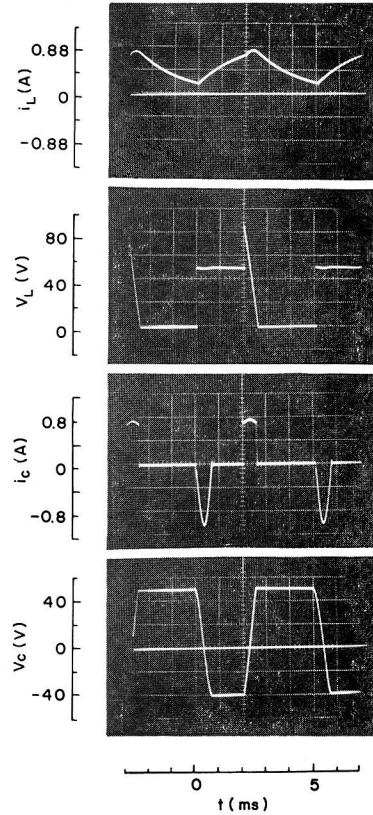


Fig. 6'. Experimental oscillograms of i_L , v_L , i_C and v_C when $C=5 \mu\text{F}$, $L_0=0 \text{ mH}$, $L_1=10 \text{ mH}$ and $r_{L0}=0 \Omega$.

Next we show several examples of numerical calculations in Figs 6, 7, 8 and 9, where

Fig. 6 : $C=5 \mu\text{F}$, $L_0=0 \text{ mH}$, $L_1=100 \text{ mH}$, $r_{L0}=0 \Omega$,

Fig. 7 : $C=10 \mu\text{F}$, $L_0=0 \text{ mH}$, $L_1=100 \text{ mH}$, $r_{L0}=0 \Omega$,

Fig. 8 : $C=5 \mu\text{F}$, $L_0=0 \text{ mH}$, $L_1=20 \text{ mH}$, $r_{L0}=0 \Omega$,

Fig. 9 : $C=5 \mu\text{F}$, $L_0=10 \text{ mH}$, $L_1=100 \text{ mH}$, $r_{L0}=1.9 \Omega$.

Also in Figs 6', 7', 8', and 9', we present the experimental oscillograms corresponding to the calculated waveforms shown in Figs 6, 7, 8 and 9 respectively.

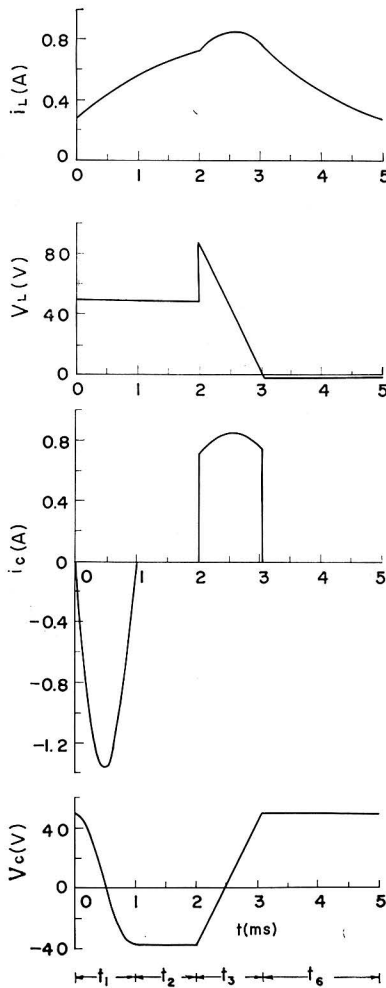


Fig. 7. Calculated waveforms of i_L , v_L , i_C and v_C when $C=10 \mu\text{F}$, $L_0=0 \text{ mH}$, $L_1=100 \text{ mH}$ and $r_{L0}=0 \Omega$.

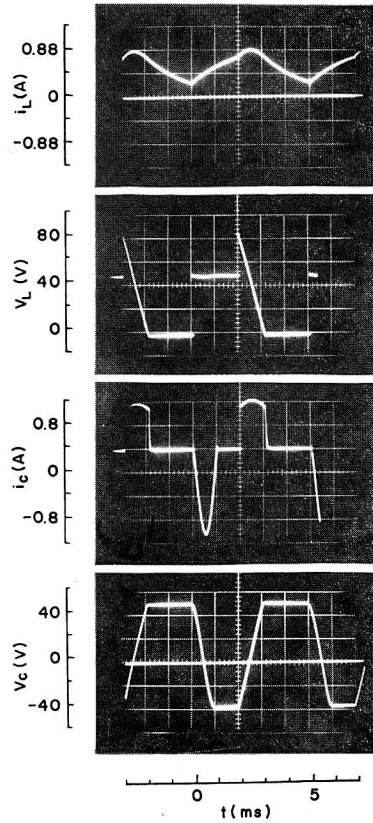


Fig. 7'. Experimental oscillograms of i_L , v_L , i_C and v_C when $C=10 \mu\text{F}$, $L_0=0 \text{ mH}$, $L_1=100 \text{ mH}$ and $r_{L0}=0 \Omega$.

4. Discussion

Comparing the waveforms by numerical calculations with ones from experimental results, we see that both correspond very much as shown in Figs 6 to 9 and 6' to 9'. The results considering the internal resistance of each element present themselves by the fact that in mode II the value of v_{C2} decreases to about 40 V, in modes I and II v_L decreases very slightly and in modes IV, V and VI v_L becomes negative.

Now in Fig.10 we show the calculated relations between the condenser capacity

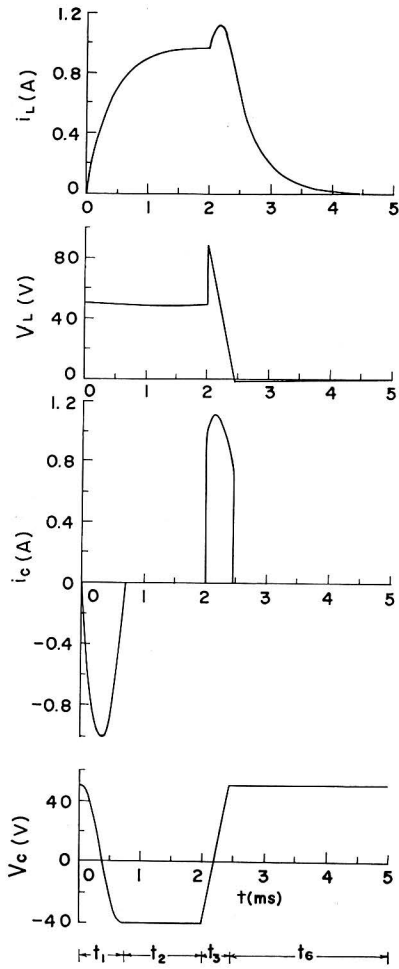


Fig. 8. Calculated waveforms of i_L , v_L , i_C and v_C when $C=5 \mu\text{F}$, $L_0=0 \text{ mH}$, $L_1=20 \text{ mH}$ and $r_{L0}=0 \Omega$.

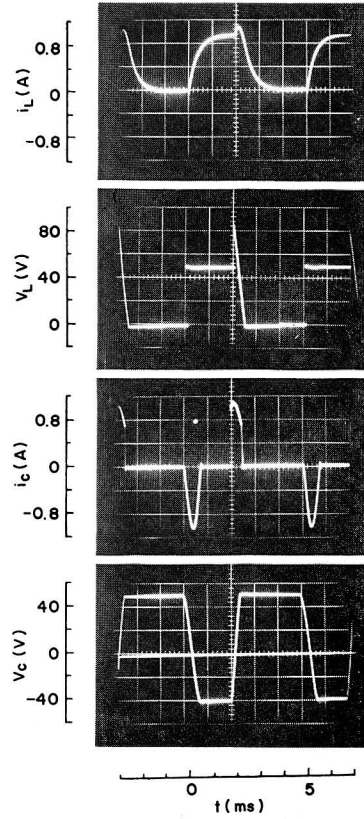


Fig. 8'. Experimental oscillograms of i_L , v_L , i_C and v_C when $C=5 \mu\text{F}$, $L_0=0 \text{ mH}$, $L_1=20 \text{ mH}$ and $r_{L0}=0 \Omega$.

C and the duration t_3 of the mode III in the case where $L_0=0$. As the load voltage waveform of an ideal chopper circuit should be a complete rectangular wave, we must make t_3 as short as possible. As mode III is the one in which $Th1$ is turned off, the following condition must be satisfied to make turn-off of $Th1$ possible, namely

$$\Delta t > t_{off}, \tag{15}$$

where

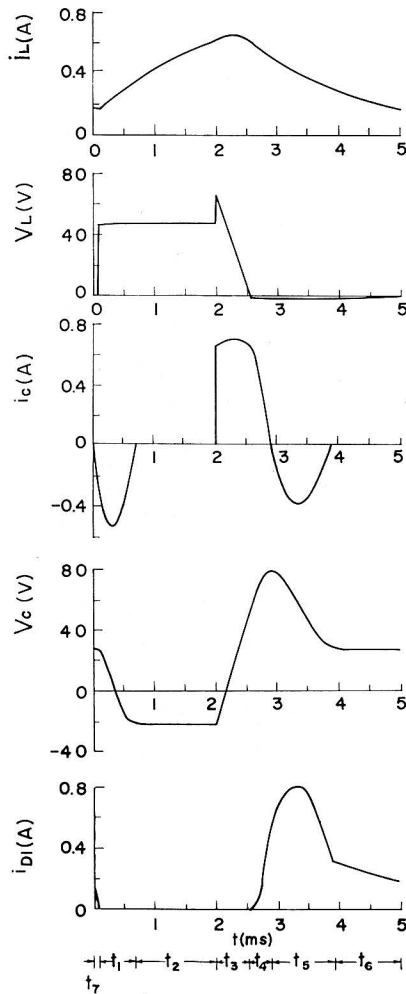


Fig. 9. Calculated waveforms of i_L , v_L , i_C , v_C and i_{D1} when $C=5\ \mu\text{F}$, $L_0=10\ \text{mH}$, $L_1=100\ \text{mH}$ and $r_{L0}=1.9\ \Omega$.

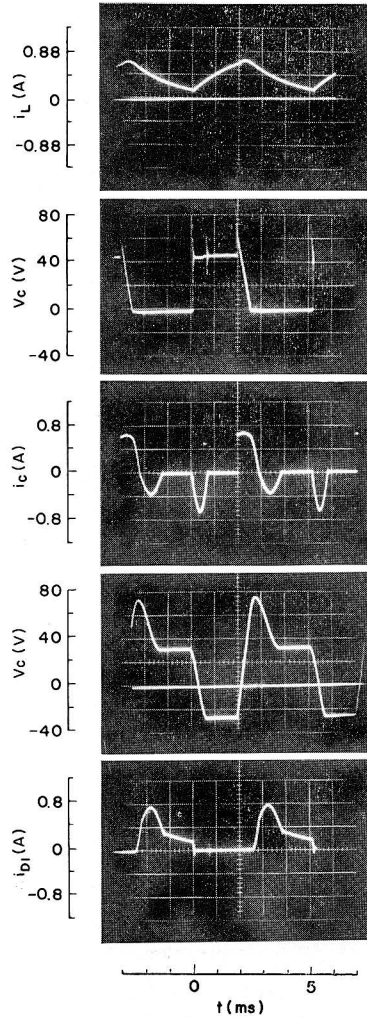


Fig. 9'. Experimental oscillograms of i_L , v_L , i_C , v_C and i_{D1} when $C=5\ \mu\text{F}$, $L_0=10\ \text{mH}$, $L_1=100\ \text{mH}$ and $r_{L0}=1.9\ \Omega$.

$$\left. \begin{aligned} t_{off} &: \text{the turn-off time of } Th\ 1, \\ \Delta t &: \text{see Fig. 11.} \end{aligned} \right\} \quad (15)$$

In the figures, v_{ci} and v_{cm} are the initial and peak values, respectively, of v_c in a stage.

On the other hand, from Fig. 10 we can find that t_3 increases when C does and also it varies with L_1 . From numerical calculation results we arrive at a relation

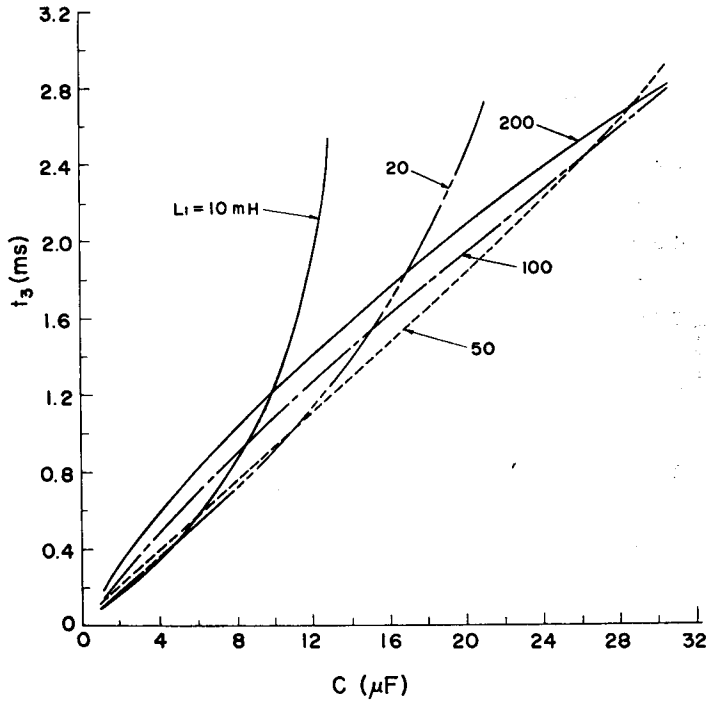


Fig. 10. Relations of t_3 vs. C .

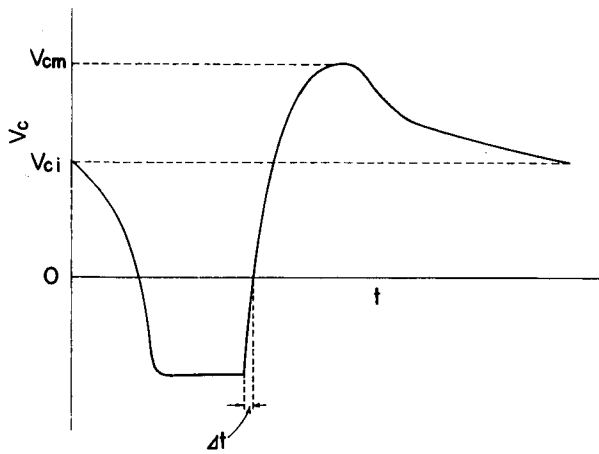


Fig. 11. u_c-t curve.

that t_3 is about twice Δt , accordingly by the characteristic curves in Fig. 10 we can determine the values of L_1 and C which makes t_3 shortest in the range, in which Eq. (15) is satisfied. In this connection, the condition of $\lambda < 1$ must be satisfied, because in the case of $\lambda \geq 1$ mode VI doesn't exist.

Now we show the calculated relations of the average load voltage V_L and current I_L vs. C in Figs 12 and 13 respectively. According to those figures, both V_L and I_L increase when L_1 and C do, because the larger C is, the larger t_s and so V_L

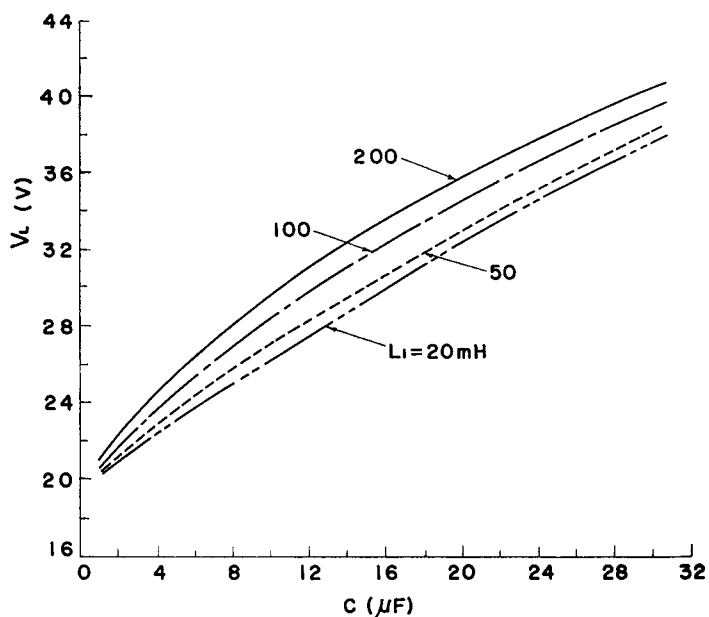


Fig. 12. Relations of V_L vs. C .

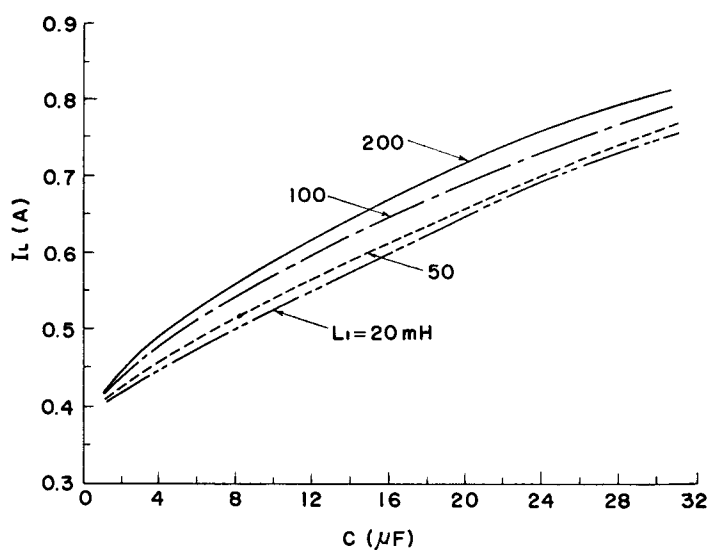
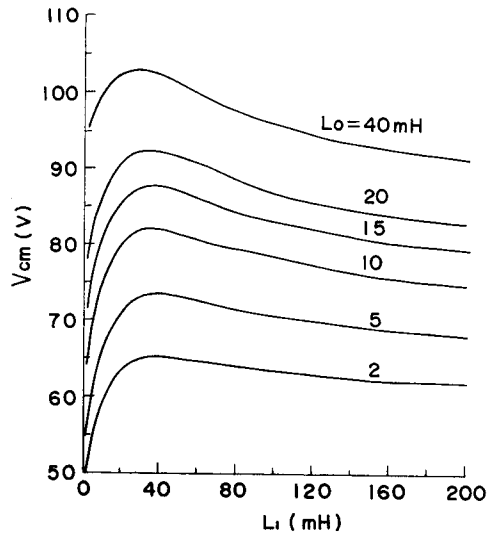


Fig. 13. Relations of I_L vs. C .

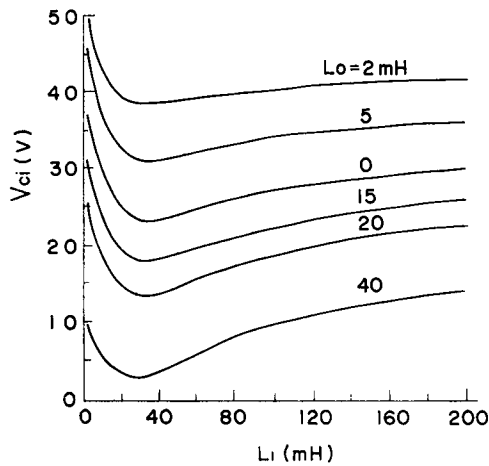
and I_L become and the larger L_1 is, the larger v_{c3}^{+0} therefore V_L becomes, and if L_1 increases, the increment of i_{L6} becomes larger than the decrements of i_{L1} and i_{L2} and therefore I_L increases. If the waveform of v_L is ideal, it is satisfied theoretically that $V_L=20V$, where V_L is given by the following conventional and simple relation,

$$V_L = ET_{on}/T. \tag{16}$$

However the practical values of V_L and I_L must be acquired from Fig. 12 and Fig. 13.



(a) $V_{cm} - L_1$



(b) $V_{ci} - L_1$

Fig. 14. Relations of v_{cm} and v_{ci} vs. L_1 .

Next, when the source consists of transformer and rectifiers, we can not avoid containing inductance in the power source, and the waveforms of the voltages and currents in such a case are shown in Fig. 9 and Fig.9'. According to the figures, when L_0 is contained, the initial inclination of v_L in mode I is not so sharp and an oscillatory phenomenon due to L_0 and C appears upon the waveform of v_c . Then we show the quantitative relations between L_1 and v_{cm} , and L_1 and v_{ci} in Fig.14 (a) and (b) respectively. According to Fig. 14, v_{cm} increases and v_{ci} decreases when L_0 increases, and concerning L_1 the tendency is most remarkable near about $20mH$ because of the resonance of L_1 and C , though the value is a little changed by the value of C . Moreover the inversed voltage of $Th 1$ must be higher than v_{cm} , and as v_{ci} decreases with the increase of L_0 , commutating failures may be sometimes induced unless enough charging voltage is given. In order to prevent them, we must adopt the means of using a thyristor instead of $D 1$ or connect large smoothing condensers to the power source.

5. Conclusion

In this paper, we have performed strict analysis about the oscillation circuit type chopper, investigated numerically and experimentally under various circuit conditions, obtained the various useful results of optimum circuit conditions and others as previously described and given several guides for chopper circuit designs.

Acknowledgement

The authors wish to express their appreciation to Mr. T. Andō in Department of Electrical Engineering.

References

- 1) K. Heumann; Commun. and Electronics **83**, 390 (1964).
- 2) W. McMurray; Commun. and Electronics **83**, 198 (1964).
- 3) B. D. Bedford and R. G. Hoft; Principles of Inverter Circuits, 332 and 348, Wiley (1964).
- 4) J. Takeuchi; SCR Circuit Theory and Applications to Motor Control, 207, Ohm (1968).
- 5) N. Sato: J.I.E.E.J., **87**, 152, Feb. (1967).
- 6) S. Hayashi; Periodically Interrupted Electric Circuits, Denki-Shoin (1961).